A New Look at Snowpack Trends in the Cascade Mountains

MARK T. STOELINGA, MARK D. ALBRIGHT, AND CLIFFORD F. MASS

Department of Atmospheric Sciences, University of Washington, Seattle, Washington

(Manuscript received 3 November 2008, in final form 25 November 2009)

ABSTRACT

This study examines the changes in Cascade Mountain spring snowpack since 1930. Three new time series facilitate this analysis: a water-balance estimate of Cascade snowpack from 1930 to 2007 that extends the observational record 20 years earlier than standard snowpack measurements; a radiosonde-based time series of lower-tropospheric temperature during onshore flow, to which Cascade snowpack is well correlated; and a new index of the North Pacific sea level pressure pattern that encapsulates modes of variability to which Cascade spring snowpack is particularly sensitive.

Cascade spring snowpack declined 23% during 1930–2007. This loss is nearly statistically significant at the 5% level. The snowpack increased 19% during the recent period of most rapid global warming (1976–2007), though this change is not statistically significant because of large annual variability. From 1950 to 1997, a large and statistically significant decline of 48% occurred. However, 80% of this decline is connected to changes in the circulation patterns over the North Pacific Ocean that vary naturally on annual to interdecadal time scales. The residual time series of Cascade snowpack after Pacific variability is removed displays a relatively steady loss rate of 2.0% decade^{-1}, yielding a loss of 16% from 1930 to 2007. This loss is very nearly statistically significant and includes the possible impacts of anthropogenic global warming.

The dates of maximum snowpack and 90% melt out have shifted 5 days earlier since 1930. Both shifts are statistically insignificant. A new estimate of the sensitivity of Cascade spring snowpack to temperature of -11% per °C, when combined with climate model projections of 850-hPa temperatures offshore of the Pacific Northwest, yields a projected 9% loss of Cascade spring snowpack due to anthropogenic global warming between 1985 and 2025.

1. Introduction

The multidecadal variation of snowpack in the Cascade Mountains of the Pacific Northwest is an issue of substantial scientific interest, societal impact, and some controversy. Major scientific issues include determining the magnitude of recent snowpack changes, the dependence of snowpack trends on the period examined, and the importance of natural climate variability versus anthropogenic global warming on past and future snowpack changes. The societal and ecological impacts of changes in Cascade Mountain snowpack are significant, since melting mountain snow provides critically needed water resources during the dry summer and early fall months for agriculture, hydroelectric production, maintenance of fish runs, and urban water supplies within the heavily populated Puget Sound and Willamette Valley corridors of Washington and Oregon.

A recent scientific report for the state of Oregon (Dodson et al. 2004) suggested that Cascade snowpack has declined nearly 50% in recent decades, with dates of annual snowpack maximum, melt out, and streamflow maximum shifting several weeks earlier. An active debate developed among the local scientific community on this issue, centered on the magnitude and origins of recent snowpack changes. These discussions have been highlighted in the local media[1] and led to the initiation of relevant new studies, including this one, focused on Cascade Mountain snowpack (e.g., Mote et al. 2008; Casola et al. 2009).

A growing body of literature has examined the multidecadal trends and variability of snowpack in the Cascade Mountains during the latter half of the twentieth century, some as part of larger studies of snowpack in western

Corresponding author address: Mark T. Stoelinga, University of Washington, Department of Atmospheric Sciences, Box 351640, Seattle, WA 98115.
E-mail: stoeling@washington.edu

[1] *Seattle Times*, 15 March 2007; *Portland Oregonian*, 24 February 2007.

DOI: 10.1175/2009JCLI2911.1

North America (Cayan 1996; Mote et al. 2005; Hamlet et al. 2005; Mote 2006; Barnett et al. 2008; Pierce et al. 2008) and others more specifically focused on the Pacific Northwest or Cascades (Mote 2003; Mote et al. 2008). These studies have found that spring snowpack in the Cascades experienced large declines (20%–40%) during roughly the latter half of the twentieth century (Mote 2003; Mote et al. 2005, 2008; Hamlet et al. 2005). It was also found that this decline was due more to warming temperatures than to decreases in precipitation (Mote et al. 2005, 2008). This conclusion was supported by the observation that percentage losses of spring snowpack were greater at low elevations than at high (Mote 2003, 2006). Related studies of spring streamflow for rivers in western North America have found a trend toward earlier spring melt pulses during approximately the same period (Cayan et al. 2001; Stewart et al. 2005; Regonda et al. 2005). Several of the above studies have suggested that a substantial portion of the observed large losses of snowpack and earlier spring streamflow pulses in the latter half of the twentieth century are due to anthropogenic global warming (Mote et al. 2005; Stewart et al. 2005; Hamlet et al. 2005; Mote 2006; Mote et al. 2008).

However, some findings in these studies make the picture less clear, both in terms of the magnitude and cause of the Cascade snowpack decline. Two studies that examined Cascade snowpack trends starting prior to 1945 (Hamlet et al. 2005; Mote et al. 2008) found much smaller losses than trends beginning around 1950. Hamlet et al. (2005), using hydrological model simulations, found that spring snowpack in the Pacific Northwest has declined only 5% from 1916 to 2003. Also, trends in Cascade snowpack since 1976, when global temperature records have shown the greatest warming, show no loss or even a slight gain (Mote 2003; Mote et al. 2005, 2008).

An important contributor to Cascade snowpack trends is the influence of natural variability in the North Pacific ocean–atmosphere system on annual to interdecadal time scales, encapsulated in various climate patterns or indices such as El Niño–Sothern Oscillation (ENSO), the Pacific–North America pattern (PNA; Wallace and Gutzler 1981), the North Pacific Index (NPI; Trenberth and Hurrell 1994), and the Pacific decadal oscillation (PDO; Mantua et al. 1997). In particular, two major shifts in the long-term phase of the PDO in 1947 and 1977 were associated with increases and decreases, respectively, in the long-term mean Cascade spring snowpack, and the latter shift may partly explain the downward trend in snowpack during the second half of the twentieth century. Several studies have regressed spring snowpack with one or more of the climate indices mentioned above to assess the contribution of natural climate variability to Cascade snowpack trends (Mote 2006; Mote et al. 2008). These studies found that such climate indices explain no more than about 40% of the observed loss of Cascade spring snowpack since 1950, with the implication that the remainder might be attributable to anthropogenic global warming. However, it is not clear that these indices are the best measure of the particular modes of natural variability of the North Pacific atmospheric circulation to which Cascade snowpack is most sensitive, and thus the influence of natural climate variability on Cascade snowpack remains an open question. A goal of this study is to examine natural variability, emphasizing the multiple modes of North Pacific circulation that most strongly affect Cascade snowpack.

Recently, Casola et al. (2009) focused on the sensitivity of snowpack to winter-mean temperature, rather than on long-term linear trends. Using geometrical, modeling, and observational approaches, they estimated the sensitivity of the Cascade spring snowpack to be a 16% loss per °C warming. Applying observed *global* temperature trends, this sensitivity suggested an 8%–16% decline in Cascade snowpack during the past 30 years, which they argue has been masked by large natural variability on annual to interdecadal time scales. Only one of their methods for estimating the sensitivity was based on the observed relationship between snowpack and temperature, and it produced a highly uncertain result because of small sample size and poor correlation between the two variables.

In this study, we develop an estimate of monthly Cascade snowpack based on a simple water balance and high-quality observations of precipitation and streamflow. This new time series extends back to 1930, allowing the examination of trends starting roughly 20 years earlier than has been reliably estimated from direct snowpack observations and, importantly, spanning both known phase shifts of the PDO rather than just one. Using this monthly time series, this paper

1) examines trends in spring snowpack amount, maximum snowpack date, and 90% melt-out date over three different time periods and compares the results to previous studies;
2) estimates the sensitivity of Cascade snowpack to lower-tropospheric temperature; and
3) reexamines the influence of natural Pacific climate variability on Cascade snowpack by seeking circulation patterns that specifically influence Cascade snowpack.

In addition, this study examines the question of how regional lower-tropospheric temperature has changed in recent decades, how it is projected to change over the next few decades by climate model projections, and the implications for the future of spring snowpack in the Cascades.

2. Data and methods

a. Streamflow data

A key component of the snowpack estimate developed in this study is a collection of long-term streamflow measurements from rivers draining undisturbed watersheds of the Cascade Mountains (Fig. 1). Most rivers within the Cascades have multiple gauging stations with records extending over many decades. Only a subset of these stations are contained within the Hydro-Climate Data Network (HCDN; Slack and Landwehr 1992), a set of U.S. gauging stations whose records have been quality controlled and are generally free of anthropogenic contamination by dams, diversions, major land-use changes within the watershed, or measurement errors. For this study, we used the seven HCDN stations within a polygon defining the Cascades (Fig. 1) that have complete monthly streamflow records spanning water years[2] 1930–2007. The starting year of 1930 was chosen because most of the HCDN gauging stations in the region began recording between 1928 and1930. The boundaries of the upstream drainage area for each gauging station are shown in Fig. 1. These drainage areas, subsequently referred to as the ''watershed subset,'' provide a representative sampling of the Cascades in the north–south direction, and include both the east and west sides of the Cascade crest. To produce a single runoff time series for the watershed subset, the monthly runoffs from the seven gauging stations are simply added together, and the total is converted to percent of the 1961–90 annual mean.

b. Precipitation data

The second key component of the snowpack estimate is precipitation derived from a subset of U.S. Historical Climate Network (USHCN; Karl et al. 1990) stations in the west side of the Cascade polygon and within 10 km of the Cascade mountains. Only precipitation from the west side of the Cascades is used because annual runoff and spring snowpack on either side of the Cascades correlates much better with west-side than east-side precipitation. This is because most of the heavy snow at high elevations on either side of the crest occurs during westerly flow, when precipitation at low-elevation stations on the west (windward) side is also maximized, but low-elevation stations on the east (lee) side are shadowed. The eight stations chosen (Fig. 1) have a complete monthly record for 1930–2007 and are well distributed in the north–south direction. Despite the tendency for stations to be at low elevations, it will be shown later that they provide a precipitation record that can be calibrated

[2] The ''water year'' is defined as 1 October through 30 September.

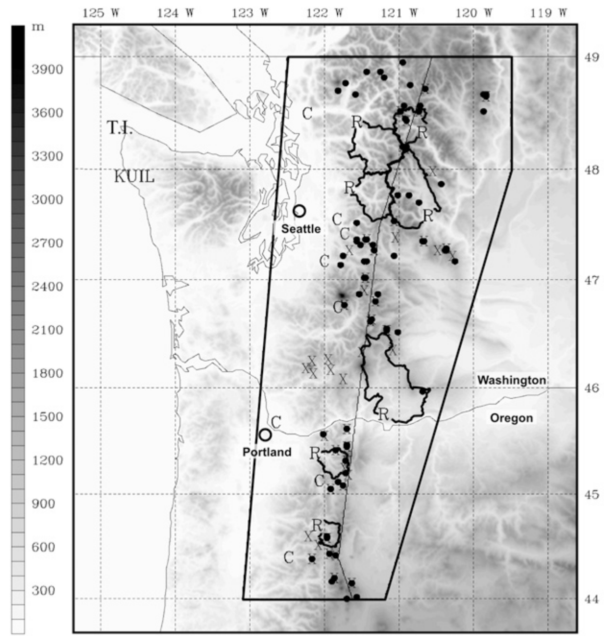

FIG. 1. Map of study area. Heavy solid polygon defines ''Cascade Mountains'' for the purposes of this study. The thin solid line divides the Cascade Mountains into west-of-crest and east-of-crest regions. Filled black dots are locations of qualifying snow course sites for the observational snowpack verification dataset, × marks qualifying SNOTEL sites, C marks qualifying USHCN temperature–precipitation sites, and R marks qualifying HCDN streamflow gauge sites, with adjacent solid curves outlining the associated watersheds (or ''watershed subset'' referred to in text). ''KUIL'' and ''T.I.'' mark the Quillayute and Tatoosh Island National Weather Service (NWS) upper-air sites used to define T_{850ons}.

to produce a total precipitation input for the watershed subset. The station precipitation values are converted to monthly percent of normal (1961–90) and then averaged among the eight stations to produce a single precipitation time series.

c. Temperature data

The monthly surface temperature records for the eight USHCN stations are used to provide a surface temperature time series for the watershed subset used in this study. As with precipitation, only west-side temperature observations are used because snowpack on both sides of the crest correlates more highly with west-side winter temperatures than with east-side winter temperatures. The temperature data are converted to anomalies from the monthly station means (1961–90), and then averaged among the eight stations to produce a single temperature time series.

The 850-hPa temperatures and winds from National Weather Service operational soundings on the Washington coast are used to determine how the snowpack is influenced by lower-tropospheric temperatures. Sounding data at Quillayute, Washington (KUIL; Fig. 1) were extracted from the quality-controlled Integrated Global Rawinsonde Archive (IGRA; Durre et al. 2006) for the period 1967–2007. From 1948 to 1966, soundings were launched from Tatoosh Island, approximately 50 km north of KUIL (Fig. 1). While there is no overlapping time period to compare the time series from these two sites, there is a USHCN surface site at Forks, Washington, nearly collocated with KUIL, with a continuous, quality controlled temperature record throughout the entire time period of interest (1930–2007). Comparison between the 850-hPa temperatures at KUIL and Tatoosh with the surface temperature record at Forks indicates that the bias between Tatoosh and Forks from the period 1948–66 is 0.4°C colder than the bias between KUIL and Forks from the period 1967–2007. Assuming that the long-term mean lapse rates at the two locations are approximately the same, this difference is consistent with Tatoosh's location 50 km north of KUIL and a mean winter-season 850-hPa meridional temperature gradient of $-0.8°\mathrm{C}\ (100\ \mathrm{km})^{-1}$ in this region. [The winter-mean meridional temperature gradient at 850 hPa was determined from a 1948–2008 November–March mean 850-hPa temperature plot created on National Oceanic and Atmospheric Administration (NOAA)/Earth System Research Laboratory's Interactive Plotting and Analysis Page (http://www.esrl.noaa.gov/psd/cgi-bin/data/composites/printpage.pl).] Therefore, we added this bias to the Tatoosh Island record to make it compatible with KUIL. We also examined the behavior of the Tatoosh Island record before and after 1957, when that site switched from a 0300–1500 UTC launch schedule to 0000–1200 UTC, and found no difference in bias with respect to Forks. Finally, 850-hPa temperatures for 1930–47 (prior to the start of upper-air observations on the Washington coast) were estimated using a linear regression between Forks surface temperatures and KUIL–Tatoosh 850-hPa temperatures from the period 1948–2007, during which these two temperature records were correlated at $r = 0.82$.

d. The water-balance snowpack estimate

This paper utilizes a monthly time series of Cascade snowpack for water years 1930–2007 that was developed by applying a simple water-balance equation to the watershed subset. This water balance relates monthly changes in snowpack in a watershed to the monthly accumulated precipitation, evapotranspiration (ET), river runoff, and soil moisture change within the watershed. The method relies on good measurements of precipitation and runoff, which dominate the monthly water balance in the Cascades, and makes reasonable assumptions about the smaller ET and soil moisture changes. The details of the method are described in the appendix. The end result is an estimated monthly time series of snow water equivalent (SWE) volume within the watershed subset from 1930 to 2007. This estimate of SWE volume will subsequently be referred to as the *water-balance snowpack*, and will be expressed as a percent of the 1961–90 mean 1 April value.

e. Directly observed snowpack

For the purpose of verifying the water-balance snowpack, the observed monthly snowpack was estimated for the watershed subset using direct observations from manual snow course and automated Snowpack Telemetry (SNOTEL) sites in the Cascades, similar to what was done for a somewhat different area by Mote et al. (2008). The snow course sites provide in situ measurements of SWE depth consistently near 1 April and less regularly near the first of other months, with a representative network of stations available from the 1950s onward (Mote 2003; Mote et al. 2008); therefore, we use the snow course observations to verify the 1 April water-balance snowpack for the period 1955–2007. The SNOTEL sites provide continuous automated measurements of SWE depth using snow pillows, and thus provide year-round first-of-the-month SWE depth. Because the SNOTEL network began in the mid-1980s, it is used to verify the monthly time series of water-balance snowpack for the period 1984–2007. The snow course and SNOTEL sites used in this analysis were subjected to selection criteria and procedures for filling in missing data similar to those described by Mote et al. (2008). The 82 snow course sites and 50 SNOTEL locations used here are depicted in Fig. 1.

A best estimate of total SWE volume within a region considers the elevation dependence of both SWE depth and areal coverage, rather than simply averaging available SWE depth observations from a variety of elevations (Mote et al. 2008). To account for the variation of areal coverage with elevation, area versus elevation curves[3] (Fig. 2a) were generated for the watershed subset using a 1-km gridded elevation dataset. Separate curves were generated for each side of the Cascade crest because they differ significantly below 1000-m elevation. SWE depth versus elevation profiles were estimated east and west of the Cascade crest (Fig. 1) by fitting lines to the SWE depth versus elevation scatterplots for all stations within those two areas. An example is shown in Fig. 2b for 1 April SWE depth at snow courses in 2006. All sites in Fig. 1 were used to produce the linear fits rather than

[3] These curves give the total horizontal area within an elevation band ($z \pm 5$ m) within the watershed subset, as a function of elevation (z). They are proportional to the vertical derivatives of the "hypsometric curves" (not shown), which represent the empirical cumulative distribution function of area versus elevation in the watershed subset.

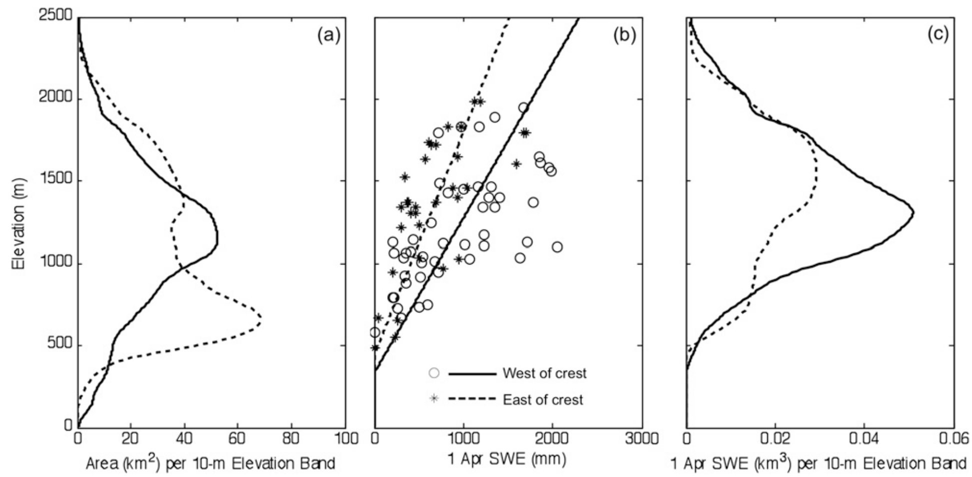

FIG. 2. Example (for 1 Apr 2006) of information used to construct the snow course–based Cascade SWE volume used to verify the water-balance snowpack. (a) Total area covered by each 10-m elevation band (equivalent to the derivative with respect to height of the hypsometric curve) within the watershed subset shown in Fig. 1. Separate curves are shown for portions of the watersheds that are west and east of the crest, as defined by the polygons in Fig. 1. (b) Scatterplot of SWE depth vs elevation, with linear fits, for stations west and east of the crest. (c) Estimate of SWE volume vs elevation within the watershed subset, obtained by multiplying (a) × (b).

just those within the watershed subset, because only a small fraction of the observing sites are actually within the watershed subset boundaries. The final steps are multiplication of the curves in Figs. 2a,b to produce profiles of east and west SWE volumes versus elevation for the watershed subset (Fig. 2c); summation with respect to elevation to produce single east and west SWE volumes; and summation of those two values to produce a final, single estimate of the total SWE volume within the watershed subset. This procedure is repeated for each year and is also applied to the monthly observed SWE at SNOTELs. The SWE volume time series are converted to percent of the 1961–90 mean 1 April value.

f. Other data issues

In several of the time series displayed, a smoothed series is shown, representing longer-term variability. The smoothing is performed using a running mean with a Gaussian-shaped weighting function, 5 years wide at half maximum and truncated at a width of 12 years.

Trends are calculated by subtracting the difference in endpoint values of the linear fit to the unsmoothed time series over the period in question. All trends for precipitation and snowpack are expressed as percentages of the 1961–90 mean value rather than of the starting value of the trend line. An important component of trend analysis of hydrologic climate parameters is the assessment of uncertainty in the calculated trends due to variability over a finite sampling time (Lettenmaier 1976; Mote et al. 2008; Casola et al. 2009). This uncertainty indicates whether a statistically significant secular trend has been detected in a finite time series. We use the formula derived by Casola et al. (2009) for determining the confidence intervals of the trends, utilizing a 95% confidence level and a two-sided test. This formula is based on the Student's t distribution and assumes that the nontrend variability is primarily Gaussian white noise. We have confirmed that the one-lag autocorrelation is small for the time series in question. However, it should be noted that even with small lagged autocorrelations, the assumption of uncorrelated annual residuals from the trend likely yields a slight underestimate of the uncertainty of the trend estimates.

3. Verification of the water-balance snowpack estimate

As a test of the water-balance snowpack estimate we compare it to the snow course and SNOTEL-derived snowpack estimates described in section 2b. Figure 3 shows a scatterplot of 1 April snowpack derived from the snow course observations for 1955–2007 (x axis) versus the 1 April water-balance snowpack (y axis). A high correlation of 0.95 is achieved, and the points lie very close to the 1:1 line. This agreement is remarkable considering the two estimates are derived from completely different observations and somewhat different watersheds. The agreement is a testament to the spatial consistency of the hydrological water balance throughout the region. The 1955–2007 linear trends from the

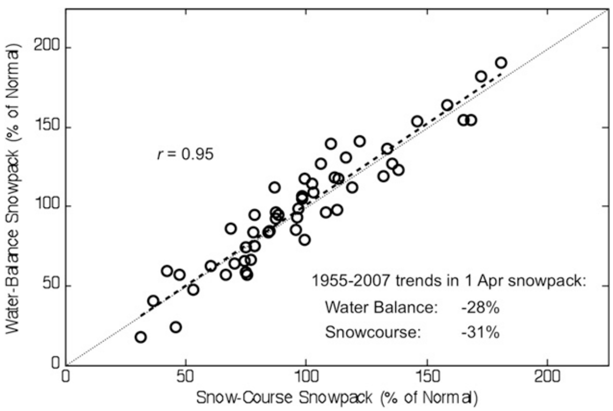

FIG. 3. Scatterplot of water-balance 1 Apr snowpack vs snow course 1 Apr snowpack, for years 1955–2007 (1955 was the first year of the snow course snowpack time series). Values are in percent of 1961–90 normal for SWE volume in the Cascade watershed subset. Also shown is the 1:1 line (thin dashed), the best-fit line (heavy dashed) with correlation, and the 1955–2007 trend values.

water-balance and snow course–based snowpack (Fig. 3) are within 3% of each other. The correlation with observed snowpack and agreement with observed snowpack trends using the water-balance approach are as good as, if not better than, those produced by hydrologic model simulations (Mote et al. 2008).

An important consideration is how well the watershed subset used to produce the water-balance snowpack estimate represents the Cascades as a whole. Although regionally averaged precipitation was used in developing the water-balance snowpack time series, the runoff observations are only from the watershed subset, and those watersheds have different characteristics than the Cascades as a whole. Specifically, the area versus elevation profile of the watershed subset (Fig. 2a) is skewed toward higher elevation than the full Cascade profile (not shown, but calculated using elevation data within the full Cascade polygon in Fig. 1). To test the potential sensitivity of the water-balance snowpack to the elevation characteristics of the watershed subset, the snow course–based snowpack time series was regenerated using the area versus elevation function for the entire Cascades. The 1955–2006 trend in 1 April snowpack calculated using the full Cascade profile was −35%, only a slightly larger decline than the −31% decline obtained using the watershed subset profile. These results instill confidence that the water-balance method applied to the watershed subset yields a snowpack estimate that is applicable to the Cascades as a whole.

One purpose of the water-balance snowpack is to exploit its monthly time resolution to examine parameters like date of maximum snowpack and melt-out date. To verify the monthly behavior of the water-balance snowpack, we compared it to the SNOTEL-derived snowpack, which also has monthly time resolution, but only for 1984–2007. The two monthly time series during this period are shown in Fig. 4. In general, the water-balance snowpack tracks the SNOTEL-estimated snowpack closely in terms of the timing and magnitude of the maxima and the annual melt out. Occasionally the water-balance snowpack exhibits some erratic small-amplitude perturbations around the time of maximum snowpack (e.g., water years 1993, 1995, and 2005), which can result in unrealistically early dates of maximum snowpack, but such years are uncommon.

Overall, these verification results provide confidence that the water-balance snowpack can be used to assess the long-term behavior of 1 April Cascade snowpack and the timing of maximum snowpack and melt out. These assessments are the subject of the next section.

4. Results

a. Snowpack trends

The full record of the water-balance snowpack on 1 April for the Cascades is shown in Fig. 5a. The unsmoothed time series shows considerable annual variability, ranging

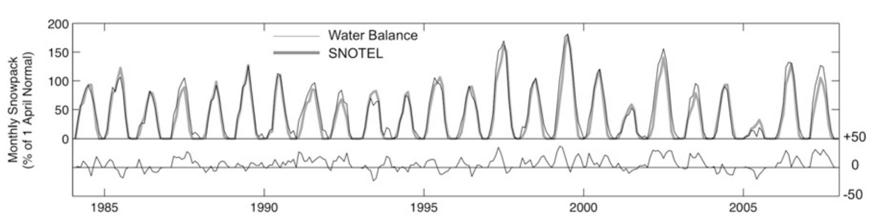

FIG. 4. (top plots) Monthly snowpack (scale at left) derived from the water-balance model (thin black) and from SNOTEL observations (heavy gray), expressed as a percent of the 1961–90 normal 1 Apr SWE volume for the watershed subset, for water years 1992 through 2007. (bottom plots) Difference (scale at right) between water-balance snowpack and SNOTEL snowpack, i.e., thin solid minus heavy gray time series in (top plot). Time axis is labeled at the first day of each water year (1 Oct of previous calendar year). Vertical scales are equal but offset.

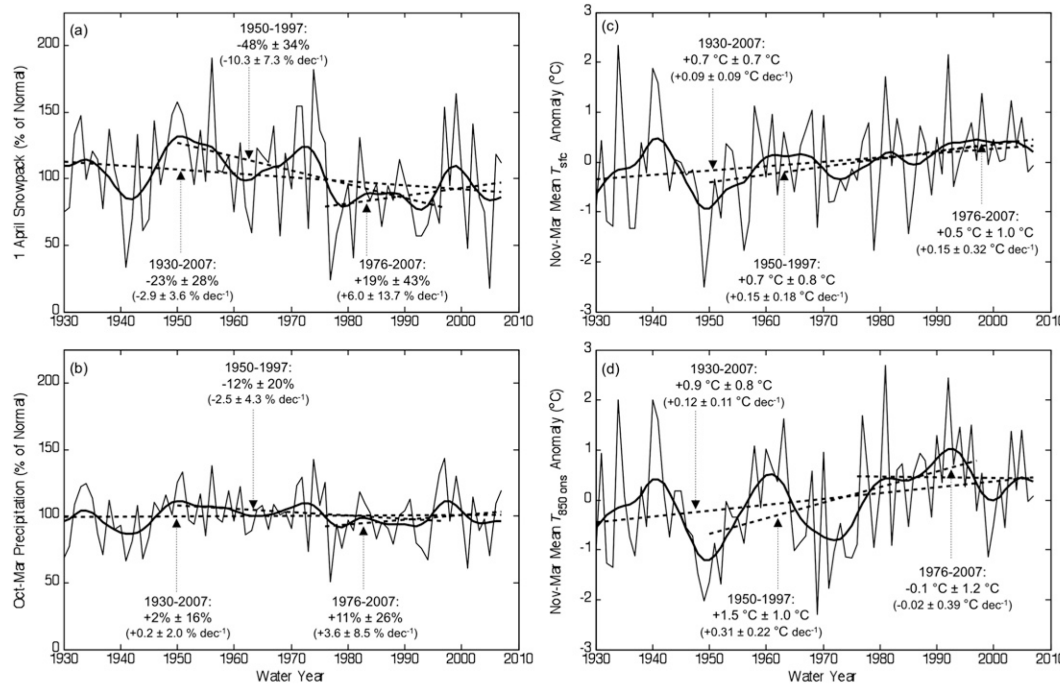

FIG. 5. (a) The 1 Apr water-balance snowpack (% of 1961–90 mean, thin solid curve); smoothed version (heavy solid curve); trend lines over the periods indicated (heavy dashed lines), with trend values (given in total percent change and percent per decade) and 95% confidence intervals listed. (b) As in (a), except for October–March west Cascade-averaged precipitation (% of 1961–90 mean). (c) As in (a), except for November–March west Cascade-averaged temperature anomaly (°C). (d) As in (a), except for November–March mean 850-hPa temperature anomaly (°C) at KUIL when 850-hPa flow is onshore. Temperature anomalies are with respect to the 1961–90 mean.

from a maximum of 191% of normal in 1956 to a minimum of 18% of normal in 2005. Trends were calculated over three periods. Over the full period of record (1930–2007), the trend is −23%, although this trend is not quite statistically significant (as indicated by the 95% confidence interval of ±28%) because of the large variability of the snowpack. The second period (1950–97) was used by Mote et al. (2005) to demonstrate large declines in snowpack over western North America. This period spans a known shift in the PDO from its "cool" to "warm" phase in 1977, when there was also a shift from a high to a low snowpack regime over the Pacific Northwest (Cayan 1996; Mantua et al. 1997). The water-balance snowpack shows a large, statistically significant decline of 48% during the 1950–97 period, much of it associated with the cool-to-warm PDO shift in 1977. Further analysis of the connection of snowpack to natural Pacific climate variability will be presented later. The third time period is 1976–2007, which is of unique interest because it is almost entirely after the cool-to-warm PDO shift of 1977, and coincides with a period of particularly rapid increase in global-mean surface temperatures, as indicated by analyses such as that of the Hadley Centre/Climatic Research Unit (Brohan et al. 2006). The most recent Intergovernmental Panel on Climate Change (IPCC) report (Solomon et al. 2007) ascribed much of this recent global warming to anthropogenic increases in greenhouse gases. In spite of the rapid global warming, this period saw a 19% *increase* in snowpack in the Cascades, although this trend falls far short of the large (43%) threshold required for statistical significance at the 5% level because of the short period and large annual variability of the snowpack.

b. *Relationship between snowpack, precipitation, and temperature in the Cascades*

Before examining the relationship of snowpack to precipitation and temperature, it is instructive to examine the relevant precipitation and temperature records. The precipitation averaged over the west side of the Cascades, accumulated from October through March (hereafter referred to as P; Fig. 5b), exhibits considerable interannual variability, though somewhat less than snowpack (Fig. 5a). The extremes are 50% of normal (1977) and 145% of normal (1997). Precipitation trends over all three time periods discussed above are small and not statistically significant. Figure 5c shows the Cascade west-side winter-averaged (November–March) surface temperature record T_s. All three periods show positive slopes. The trend during the entire period of record (+0.08°C decade^{-1}, 1930–2007) is similar to that of the winter (November–March) global-mean surface temperature[4] over the same period (+0.08°C decade^{-1}, not shown). However, whereas the global-mean warming accelerated from a rate of +0.09°C decade^{-1} during 1950–97 to +0.19°C decade^{-1} during 1976–2007, the local Cascade temperature increased more steadily at a rate of +0.09°C decade^{-1} during both periods.

In their analysis of the sensitivity of Cascade snowpack to winter-mean temperature, Casola et al. (2009) point out that the best temperature to use is one that is applicable to the location where precipitation is occurring, weighted for periods when it is occurring. They refer to this hypothetical precipitation-weighted average surface temperature as T_w. Our winter-mean T_s is a simple November–March average of temperatures at climate network stations that are, for the most part, at the foot of the mountains, rather than at high elevations where heavy snow falls. Not only are nonprecipitating periods included, but surface air temperatures at the foot of the mountains likely experience different surface energy balance regimes than in the mountains themselves. Therefore, winter-mean T_s is probably not the best estimate of T_w. Since much of the winter precipitation in the Cascades falls when cold, moist westerly to northwesterly flow in the lower troposphere impinges directly on the Cascade barrier, a better estimate of T_w might be the winter-mean temperature at 850 hPa (roughly 1500 m above sea level) for periods when the 850-hPa flow has an onshore component ($T_{850\mathrm{ons}}$). The flow direction discriminator is an attempt to weight the temperature for periods of precipitation, and use of the upstream 850-hPa level is based on our hypothesis that, during cloudy precipitating periods in the mountains, surface energy exchange in the mountains is minimal and the upstream free-atmosphere temperature probably correlates well with the mountain surface air temperature at high elevations where snow is actually falling. A time series of $T_{850\mathrm{ons}}$ (Fig. 5d) shows many of the variations seen in the T_s record, but with several important differences, including more pronounced interdecadal features, like the steep increase for 1950–97, and little trend during the recent period of rapid global warming (1976–2007). It will be shown later that these temporal characteristics reflect the interdecadal-scale climate variability of the northern Pacific Ocean.

Scatterplots of 1 April snowpack with winter precipitation, surface temperature, and 850-hPa temperature during onshore flow, along with correlations, are shown in Fig. 6. The higher correlation with precipitation (0.80) than with surface temperature (−0.44) is consistent with results of Mote (2006) and Mote et al. (2008). A substantially larger correlation is obtained with $T_{850\mathrm{ons}}$ ($r = -0.67$) than with T_s ($r = -0.44$), suggesting that $T_{850\mathrm{ons}}$ provides a better estimate of the winter temperature relevant to Cascade snowpack than does T_s.

Mote (2006) and Mote et al. (2008) used multiple linear regression to analyze the separate contributions of winter temperature and precipitation to changes in 1 April SWE depth observed at snow courses in western North America. A similar analysis is performed here, using the water-balance snowpack estimate for the Cascades. Specifically, multiple linear regression is used to find the best fit of the following linear relationship between the snowpack, precipitation, and temperature data:

$$S = (a_1P + a_2T + a_3) + S_{\mathrm{res}} = S_{\mathrm{fit}} + S_{\mathrm{res}}. \qquad (1)$$

The a terms are the regression coefficients, including the intercept a_3. The regression model produces S_{fit}, an estimate of the total snowpack S. The part of the total snowpack that is uncorrelated with the predictor variables, the "residual," is designated S_{res}. Using P and $T_{850\mathrm{ons}}$ as predictors, multiple linear correlation yields an S_{fit} that correlates with S at $r = 0.90$.

The multiple linear regression results are shown in Table 1. Over the full period of record (1930–2007), most of the 23% decrease in snowpack is associated with warming temperature. Warming plays an even larger role in the large decline in snowpack during 1950–97, and the decline is enhanced by decreasing precipitation during this period. However, during the period of recent rapid global warming (1976–2007), the slight decline in $T_{850\mathrm{ons}}$ (Fig. 5d) results in little temperature contribution to snowpack changes, leaving the increasing precipitation to dominate and produce an increase in snowpack. Examination of the residual for all three periods indicates a nontrivial contribution to the trend in 1 April snowpack (ranging from −13% to +5%)[5] due to random errors or nonlinear relationships in all three measurements and the exclusion of other factors, as discussed by Mote et al. (2008).

[4] These trends are from the monthly global-mean surface temperature time series provided by the Hadley Centre/Climatic Research Unit, described in Brohan et al. (2006).

[5] The residual produced during the full period of record (1930–2007) when using $T_{850\mathrm{ons}}$ in the multiple linear regression (−11% of normal snowpack, Table 1) was less than that produced when using T_s (−16% of 1961–90 mean snowpack, not shown), further supporting the choice of $T_{850\mathrm{ons}}$ as a more relevant temperature parameter for spring snowpack in the Cascade Mountains.

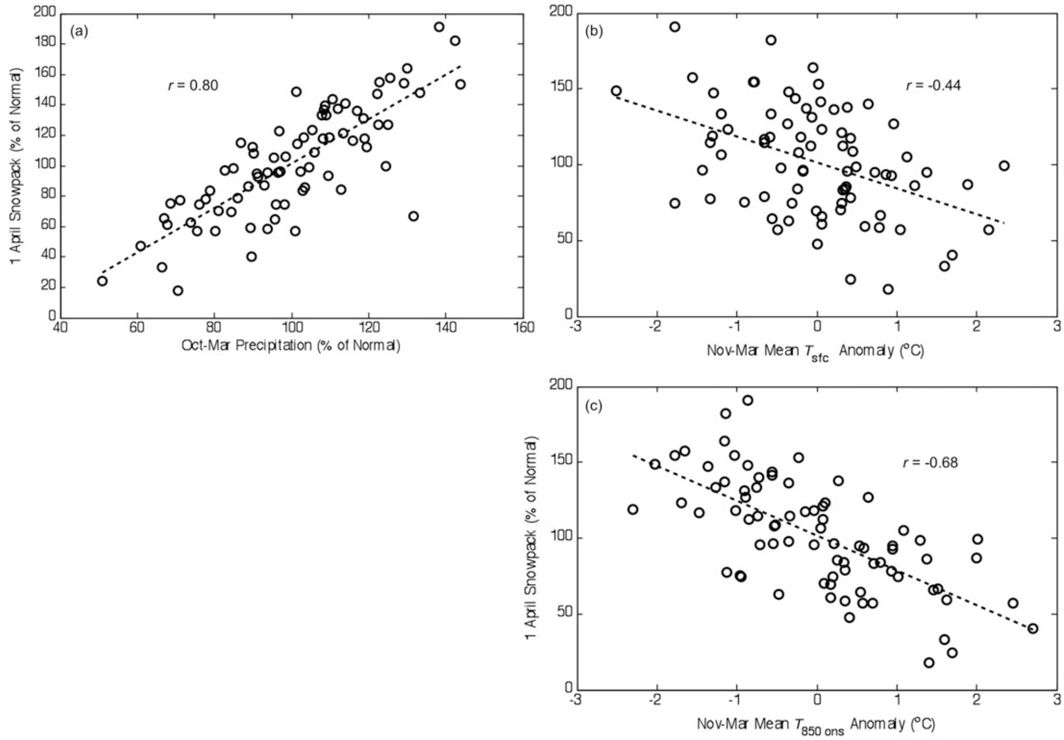

FIG. 6. (a) Scatterplot of water-balance 1 Apr snowpack vs October–March west Cascade-averaged precipitation (both as % of 1961–90 mean). (b) Scatterplot of water-balance 1 Apr snowpack vs November–March west Cascade-averaged temperature anomaly (°C). (c) Scatterplot of water-balance 1 Apr snowpack vs November–March mean 850-hPa temperature anomaly (°C) at KUIL when 850-hPa flow is onshore.

As mentioned previously, Casola et al. (2009) examined the sensitivity of the Cascade snowpack (S) to a unit change in mean winter temperature (T), expressed as percent change in S per unit change in T. They defined this sensitivity as

$$\lambda = \frac{dS}{dT} = \frac{\partial S}{\partial T} + \frac{\partial S}{\partial P}\frac{dP}{dT} = \lambda_{\text{direct}} + \lambda_{\text{feedback}}. \qquad (2)$$

In other words, the total sensitivity is the sum of the direct sensitivity to temperature (T) holding precipitation (P) constant, and any feedback due to a relationship between T and P. They estimated λ_{direct} by four different methods, finding an average value of 20% °C^{-1}. Minder (2010) found a similar result using two simple models driven by sounding observations. Of these six methods, only Casola et al.'s regression of observed S vs. T used actual snowpack observations, and that estimate had large uncertainty due to a short period of record (1970–2006) and low correlation between S and T ($r = -0.52$). Here we repeat this approach using $T_{850\text{ons}}$ and the longer period of the water-balance snowpack time series. By definition, λ_{direct} is the regression coefficient for $T_{850\text{ons}}$ produced by multiple linear regression of S with $T_{850\text{ons}}$ and P, since that regression coefficient is the slope of S with respect to $T_{850\text{ons}}$ holding P constant. By this definition, $\lambda_{\text{direct}} = -15\%$ °C^{-1}. To calculate the 95% confidence interval on the sensitivity, we use the partial correlation (Panofsky and Brier 1963) of $T_{850\text{ons}}$ and S holding P constant ($r_{\text{partial}} = -0.68$), and the same Casola et al. (2009) formula for confidence intervals discussed previously. This yields a 95% confidence interval of ±4%, considerably smaller than that obtained by Casola et al. Our smaller uncertainty is due to a longer period of record, better partial correlation of S with

TABLE 1. Trends in 1 Apr snowpack associated with terms in the multiple linear regression of 1 Apr snowpack with winter precipitation (P) and winter 850-hPa temperature during onshore flow ($T_{850\text{ons}}$).

	Snowpack change (%)		
	1930–2007	1950–97	1976–2007
Actual trend	−23	−48	+19
P part only ($T_{850\text{ons}}$ held constant)	+2	−14	+13
$T_{850\text{ons}}$ part only (P held constant)	−13	−22	+1
Full regression equation	−12	−36	+14
Residual	−11	−13	+5

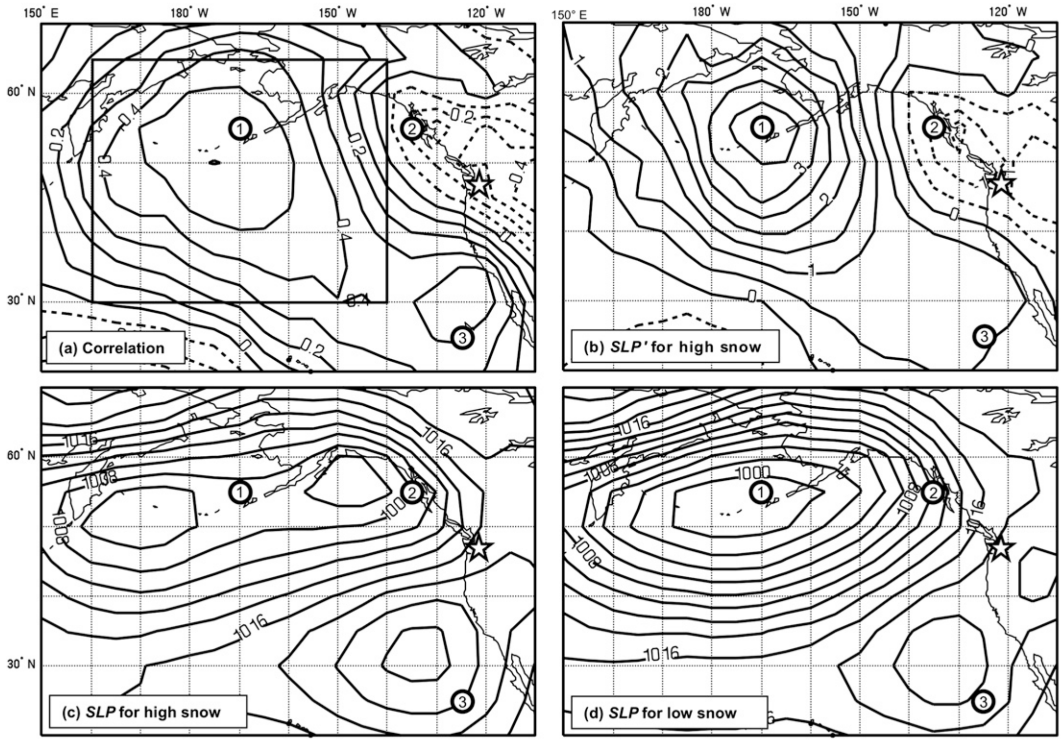

FIG. 7. (a) Map of the regression coefficient between the winter (November–March mean) sea level pressure field over the North Pacific Ocean region and the Cascade 1 Apr snowpack (from the water balance). Location of Cascade Range indicated by star. Numbered circles indicate the set of three points within the domain whose SLP explains more of the variance in snowpack than any other set of three points. Box shows averaging area for the NPI. (b) Composite of the winter SLP anomaly field (hPa, as a departure from the 1961–90 mean) during the five years with highest CSC index. (c) Composite of the total winter SLP field (hPa) during the five years of highest CSC index. (d) Composite of the total winter SLP field (hPa) during the five years of lowest CSC index.

$T_{850\mathrm{ons}}$ than with T_s, and elimination of precipitation-induced variability using multiple linear regression. Adding in the Casola et al. estimate that $\lambda_{\mathrm{feedback}}$ may be as high as $+4\%\ {}^{\circ}\mathrm{C}^{-1}$ yields $\lambda = -11 \pm 4\%\ {}^{\circ}\mathrm{C}^{-1}$, a somewhat lower estimate of the sensitivity than that given in Casola et al. ($-16\%\ {}^{\circ}\mathrm{C}^{-1}$). One caveat is that there is little understanding of how global warming has or will produce more complicated climate responses such as changes in storm intensities, storm tracks, natural modes of variability such as ENSO and PDO, etc. All of these unknowns add to the uncertainties in the magnitude, and perhaps even the sign, of $\lambda_{\mathrm{feedback}}$.

c. *Relationship between Cascade snowpack and natural interdecadal-scale variability*

The NPI (Trenberth and Hurrell 1994) is an atmospheric index that is thought to encapsulate much of the atmospheric variability associated with the PDO, as well as ENSO. It is defined as the mean sea level pressure (SLP) (minus 1000 hPa) in the north-central Pacific Ocean (see box in Fig. 7a), and can be considered a measure of the strength of the Aleutian low. It can be argued that the PDO reflects primarily natural climate variability, supported by the fact that the linear trend of the NPI explains less than 3% of its variance during 1930–2007, compared to, for example, the global surface temperature, whose linear warming trend explains over 50% of its variance during the same period. Some studies have suggested that the amplitude and frequency of ENSO, to which the PDO is closely related, are influenced by anthropogenic global warming, but this question is a matter of ongoing debate (Guilyardi 2006). A recent study by Meehl et al. (2009) argues that the PDO shift in 1977 was largely the result of anthropogenic global warming, but multiple interpretations of their experiments are possible.

Mote (2006) and Mote et al. (2008) have concluded that natural climate variability explains only about 40% of the losses in Pacific Northwest spring snowpack during the latter half of the twentieth century, based on linear regression of snowpack with the NPI and removal of its influence from the snowpack time series. We performed a similar analysis with the water-balance snowpack and obtain a similar result: the loss during 1950–97 is reduced from 48% to 29% (a relative reduction of 39.6%).

However, significant annual to interdecadal variability remains in the residual snowpack time series (not shown), suggesting that the NPI is an imperfect index of the natural Pacific climate variability that is relevant specifically to Cascade snowpack. It is entirely reasonable to suspect that there are multiple modes of natural climate variability in the North Pacific that affect Cascade snowpack that cannot be represented by a simple box average of SLP over the north-central Pacific Ocean. Such modes may not explain a large fraction of atmospheric variability over the globe or even over the North Pacific basin, but may exert a strong influence on a regional parameter such as spring snowpack in the Cascade Mountains.

To investigate this hypothesis, we sought an alternate SLP-based North Pacific atmospheric circulation index that includes multiple modes of Pacific climate variability to which Cascade snowpack is particularly sensitive. Using the gridded historical monthly mean SLP dataset (5° × 5° resolution) produced by the Hadley Centre (Allan and Ansell 2006), we constructed a map over the North Pacific Ocean of the regression coefficient between November–March mean SLP and 1 April Cascade snowpack during the period 1930–2007 (Fig. 7a). The most prominent ''center of action'' in this map is a high positive correlation with SLP within the Aleutian low (high SLP = weak Aleutian low = high Cascade snowpack) centered near 50°N, 175°W. This is the same connection between Cascade snowpack and North Pacific circulation that is captured by the winter-mean NPI (defined as the average SLP within the box in Fig. 7a). However, there are clearly two other centers of action closer to the West Coast: a region of negative correlation (low pressure = high Cascade snowpack) extending from the Alaska Panhandle southeastward into the northwestern United States, and a region of positive correlation (high pressure = high Cascade snowpack) off the coast of Southern California. The two West Coast centers of action make sense in that they both contribute to a stronger cross-barrier geostrophic flow in the Cascades.

To what degree do these three centers of action represent independent modes of variability? To investigate this question, a method was devised to identify the three points within the domain of Fig. 7a that are maximally independent from each other but also maximally correlated with Cascade snowpack (via multiple linear regression). The method is similar to the technique described by van den Dool (2007), called ''empirical orthogonal teleconnections, 2'' (EOT2). First, the grid point with the highest correlation of SLP to Cascade snowpack was identified as ''point 1,'' representing the first center of action. Using linear regression, the influence of SLP at point 1 was then removed both from the snowpack time series and from the SLP time series at all other grid points, and a new correlation map between the residual snowpack time series and the remaining SLP field was produced. The new point of highest correlation was identified as ''point 2,'' which was near the second center of action. The procedure was repeated again to find ''point 3,'' roughly near the third center of action as expected. The procedure could have been repeated to find points 4, 5, etc., but it was found that little additional variance in snowpack was explained beyond the third point. The final three points obtained[6] are those shown in Fig. 7, located at 50°N, 170°W; 50°N, 135°W; and 20°N, 125°W.

The total correlation of snowpack with SLP using the three points (via multiple linear regression) is $r = 0.84$ ($r^2 = 0.71$), and the additional fractional variance explained by incrementally adding each point to the multiple regression is 0.35, 0.24, and 0.12, respectively. In other words, the second (Alaska Panhandle) and third (California) points together explain about the same amount of variance as the first point (Aleutian low, similar to NPI). SLP time series at the three points are not highly correlated with each other ($r_{12} = 0.36$, $r_{23} = 0.04$, and $r_{31} = 0.11$), confirming that they describe essentially linearly independent modes of variability. We also performed a leave-one-out cross-validation (LOOCV) analysis on the method. By incrementally increasing the number of predictor points, LOOCV showed that the test-set error decreased for additional points up to the third point and then started to increase for four or more points, confirming that three points is the correct number to use. The fraction of explained variance of the test set was 0.66, only slightly less than the variance explained using the full dataset for both training and testing (0.71). Finally, the locations of the three points in the LOOCV trials were the same as in the original experiment, except in 13 of the 78 trials, in which one or two of the points were at most one grid point away from the originally determined locations, indicating that the three locations are robust and stable.

The result of the multiple linear regression applied to the winter-mean SLP time series at the three ''best'' points identified above can be used to construct a ''Cascade Snowpack Circulation'' index, referred to hereafter as the CSC index, to distinguish it from the NPI:

[6] It is possible that point 1 could change if it is re-identified after points 2 and 3 are known and accounted for, so a refinement procedure was applied to each of the three points in sequence to insure that they were each at the point of maximum correlation between SLP and snowpack when the influence of SLP at the other two points was removed from the snowpack and SLP time series.

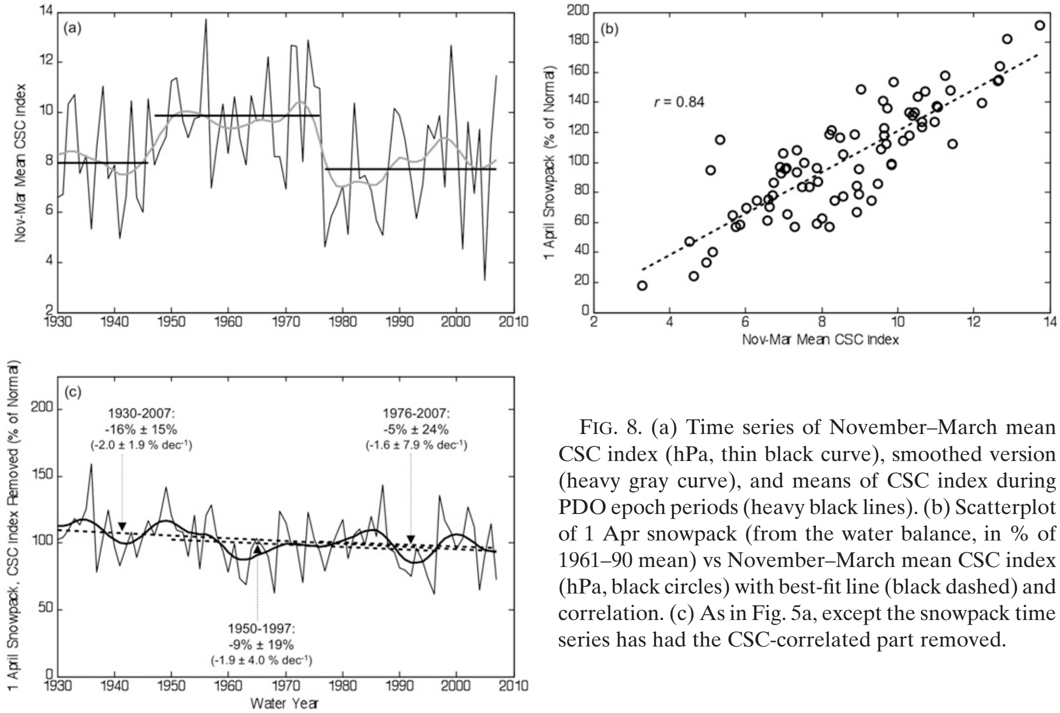

FIG. 8. (a) Time series of November–March mean CSC index (hPa, thin black curve), smoothed version (heavy gray curve), and means of CSC index during PDO epoch periods (heavy black lines). (b) Scatterplot of 1 Apr snowpack (from the water balance, in % of 1961–90 mean) vs November–March mean CSC index (hPa, black circles) with best-fit line (black dashed) and correlation. (c) As in Fig. 5a, except the snowpack time series has had the CSC-correlated part removed.

$$\text{CSC index} = 0.5985\text{SLP}_1 - 0.7349\text{SLP}_2 + 1.8382\text{SLP}_3 - 1724.8\,\text{hPa}, \tag{3}$$

where the SLP values are in hPa.

To help understand how the CSC index, as defined in (3), relates to snowpack in the Cascades, Fig. 7b shows a composite of the anomaly of the winter-mean SLP field in the 5 years with the highest CSC index during 1930–2007. The composite SLP anomaly field roughly mirrors the correlation map (Fig. 7a) and resembles the negative of a composite winter 700-hPa anomaly pattern for low 1 April snowpack years in Oregon found by Cayan (1996). A weak Aleutian low (high SLP anomaly) is coupled with low pressure along the west coast of Canada and higher pressure off Southern California. The composite SLP anomaly for the 5 years of lowest CSC index (not shown) is essentially equal and opposite of Fig. 7b. Also shown are the full winter-mean SLP field during the five highest (Fig. 7c) and lowest (Fig. 7d) CSC index years. In high index–snowpack years, the SLP field offshore of the Pacific Northwest is characterized by nearly zonal geostrophic flow that impinges directly onto the Pacific Northwest coast. In low index–snowpack years, the geostrophic flow is stronger offshore, but the flow follows a southwest-to-northeast course toward the Alaska Panhandle, bypassing the Washington–Oregon Cascades and leaving them in a more quiescent and warmer regime.

An annual time series of the winter-mean CSC index is shown in Fig. 8a, with mean values during the PDO epochs shown by horizontal bars. The CSC index shows pronounced PDO epoch transitions at 1947 and 1977, more so than the NPI (not shown), whose PDO epoch transitions are more subtle. A scatterplot of 1 April Cascade snowpack versus CSC index (Fig. 8b) illustrates the close correspondence between the two variables, and a time series of 1 April Cascade snowpack after the influence of the CSC index is removed (Fig. 8c) shows a highly reduced variability compared to the full snowpack time series (Fig. 5a). Furthermore, the residual trends in 1 April snowpack over the shorter 1950–97 and 1976–2007 periods (listed in Fig. 8c) become very consistent with the trend during the full period, unlike the full snowpack times series. The residual trend shows a remarkably steady loss of snowpack at a rate of ~2.0% decade^{-1}. We postulate that it is this residual trend in Cascade 1 April snowpack that may be due in part to the effects of anthropogenic global warming.

d. Trends in maximum snowpack date and melt-out date

Recently Hamlet et al. (2005) carried out simulations with the Variable Infiltration Capacity (VIC) hydrology model (Liang et al. 1994) over western North America for the twentieth century and found that in *some* locations, including several in the Cascades, the date of maximum snowpack has moved 15–45 days earlier in the year, and that the date of 90% melt out has shifted 15–40 days earlier. However, these results were for the small subset of points that showed the largest shifts to earlier dates. Here we examine whether such large shifts toward earlier maximum snowpack and melt out are evident in our water-balance snowpack record for several watersheds in the Cascade Mountains from 1930 to 2007.

The estimation of daily maximum snowpack and melt-out dates from the monthly snowpack time series requires an interpolation from first-of-month data to a daily time series, which is accomplished with a cubic spline interpolation.[7] Melt out is defined here as in Hamlet et al. (2005), that is, the Julian date at which each year's snowpack is reduced by 90% of that year's peak value. The maximum snowpack date and melt-out date time series, based on the water-balance snowpack, are shown on the same graph with Julian date on the *y* axis (Fig. 9), with the trends and uncertainties given for the three time periods. Both dates exhibit considerable annual variability, especially the melt-out date. The dates of both maximum snowpack and 90% melt out occur just 5 days earlier in 2007 than they did in 1930, with the threshold for a statistically significant change being two weeks. Shifts of these dates during 1950–97 are larger (tending toward earlier maximum and melt out). These results are consistent with findings of earlier spring streamflow pulse during approximately the same period (Cayan et al. 2001; Stewart et al. 2005; Regonda et al. 2005), a time interval that is strongly influenced by Pacific variability, as demonstrated in the previous section. Trends during the recent period of accelerated global warming (1976–2007) are for *later* maximum snowpack and melt-out dates, though uncertainty in the linear trend during this period is much larger than the trend itself, as was true for 1 April snowpack. The magnitudes of all the trends are reduced when the influence of the CSC index is removed from the time series (not shown).

[7] The use of a cubic-spline interpolation to convert a monthly to a daily time series of snowpack potentially can introduce error into the time series and additional uncertainty into the trends for dates of maximum snowpack and melt out. We tested this error using a SNOTEL time series with daily resolution, comparing it to time series interpolated from a monthly sampling and found that the error in melt-out date is random with a standard deviation of 5.5 days. This translates to an additional uncertainty (at the 95% confidence level) of ±4 days in the trend of melt-out date from 1930 to 2007, which is considerably smaller than the variability-induced uncertainty listed in the upper-left part of Fig. 10 (±20 days).

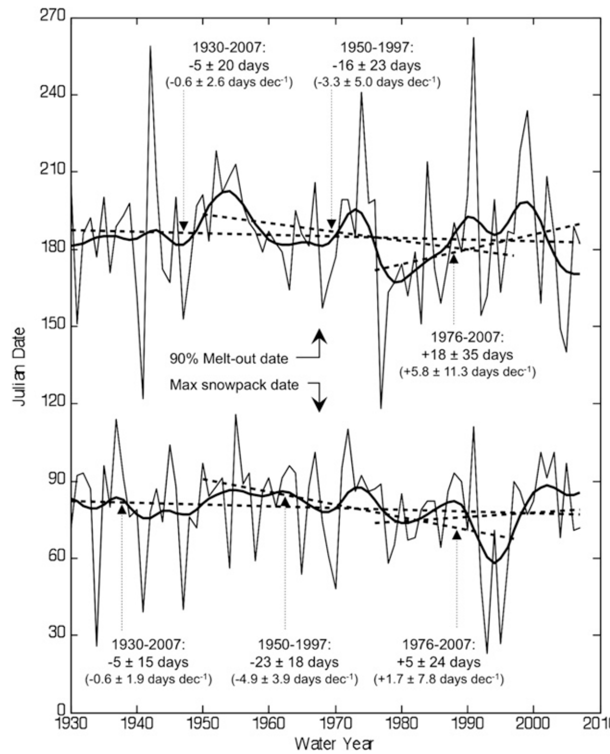

Fig. 9. As in Fig. 5a, except showing Julian date of maximum snowpack (lower curves and lines) and of 90% melt out (upper curves and lines), based on the water-balance monthly snowpack record.

5. Relationship of Cascade snowpack to past and future regional temperature changes

Section 4 showed that the temperature of lower-tropospheric onshore flow is highly correlated with the buildup of the Cascade snowpack during winter storms. This is consistent with conventional knowledge that much of the snowfall in the Cascades occurs during a synoptic-scale regime of strong westerly (cross barrier) flow in the lower troposphere, which is usually accompanied by an ideal combination of cold temperatures, plentiful moisture, and weakly stable lapse rates. The 850-hPa winter temperature during onshore flow exhibited little trend during the recent period of rapid global warming (Fig. 5d). This flat trend, although rendered uncertain by large annual variability in the time series, is nonetheless consistent with weak surface air temperature trends over a broad region of the northeastern Pacific Ocean offshore of the Pacific Northwest, as seen in a map of the 1976–2007 trends in December–February mean surface air temperature (Fig. 10) produced using the global surface temperature dataset of Hansen et al. (2001). This broad region of relatively small temperature trend offshore of the Pacific Northwest, compared to larger increases elsewhere in the Northern Hemisphere, has likely

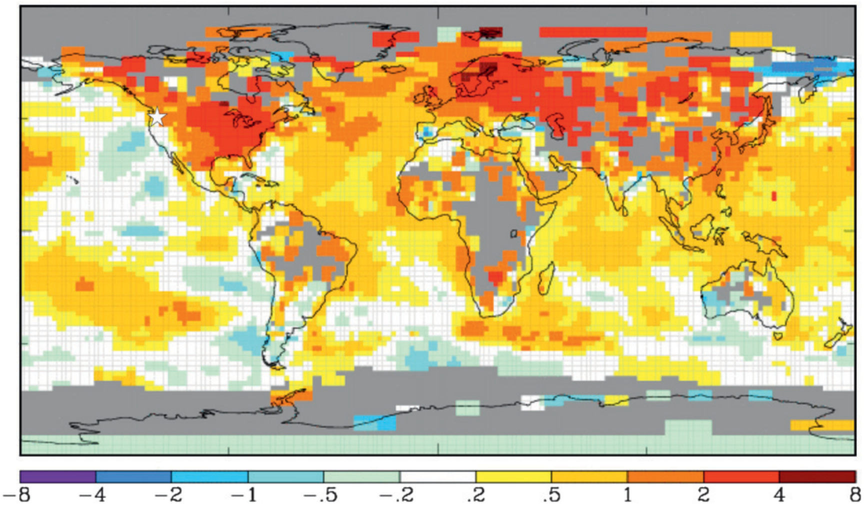

FIG. 10. Changes in December–February mean surface air temperature (°C) during the period 1976–2007, based on linear trends. The plot was generated using the temperature trend mapping web page provided by the National Aeronautics and Space Administration (NASA) Goddard Institute for Space Studies (http://data.giss.nasa.gov/gistemp/maps), which uses the surface temperature dataset described by Hansen et al. (2001). The white 5-point star indicates the region of interest in the present study.

contributed to a lack of decline in Cascade snowpack since 1976.

Casola et al. (2009) have promoted the idea of projecting future changes in Cascade spring snowpack by multiplying the estimated sensitivity with a projection of temperature change based on climate model projections. Recently, Overland and Wang (2007) examined the ensemble of coupled ocean–atmosphere climate model simulations used in the IPCC Fourth Assessment Report (AR4) (using the A1B emission scenario), and identified a group of models that best captured the observed decadal-scale variability over the northeastern Pacific Ocean during the twentieth century. Figure 11 shows the pattern of the projected change in mean November–March temperatures over the northern Pacific Ocean during 1990–2025 in Overland and Wang's ensemble, for the sea surface, surface air, and air aloft (850 hPa). All three of these temperature trend patterns suggest that the region offshore of the Pacific Northwest will continue to warm at a slower pace than most other areas around the Pacific basin. However, it can also be seen that projected warming at 850 hPa is generally larger than at the surface. The projected 850-hPa temperature change at the Washington coast from 1990 to 2025 (+0.75°C, or 0.21°C decade^{-1}) is close to the global-mean surface temperature change projected over the same period by the IPCC (+0.80°C, or 0.23°C decade^{-1}). It is also about twice the rate of warming of $T_{850\text{ons}}$ observed from 1930 to the present (+0.12°C decade^{-1}, Fig. 5d). Applying the 850-hPa warming rate of 0.21°C decade^{-1} projected by Overland and Wang's ensemble, and the snowpack sensitivity derived in section 4b of −11% °C^{-1}, yields a loss for the next few decades of around −2.3% decade^{-1}. An estimate of cumulative loss of Cascade snowpack from 1985 to 2025 that is potentially due to global warming can be projected by starting with the loss not attributable to circulation changes that has already occurred through 2007 (−2.0% decade^{-1}, section 4c) × 2.2 decades = −4.4%. To this is added the projected additional loss of 2.3% decade^{-1} × 1.8 decades (2007–25) = 4.1%, for a total of 9%. This is considerably smaller than the 29% loss from 1985 to 2025 recently projected for the Washington Cascades and Olympics in the *Washington Climate Change Impacts Assessment* (Elsner et al. 2009, chapter 3), based on hydrologic model simulations driven by a downscaled climate model ensemble.

6. Conclusions

In this study, we have considered the trends in snowpack and related parameters in the Cascade Mountains from 1930 to 2007. A major tool has been a simple water-balance method for estimating monthly Cascade Mountain snowpack from high-quality streamflow and precipitation measurements. This snowpack estimate extends back to 1930, well before the start of reliable direct snowpack observations, and also well before the large 1947 shift in the Pacific decadal oscillation (PDO). The water-balance snowpack record was analyzed in terms of its trend over various time periods, its relationship to temperature,

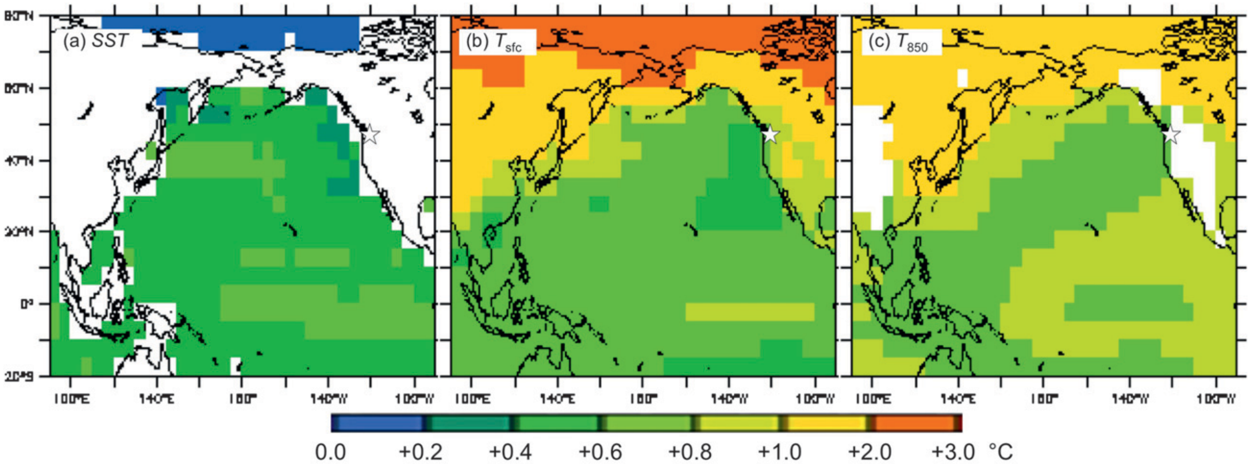

FIG. 11. Predicted linear trend of November–March mean temperature for 1990–2025 (°C), as predicted by the Overland and Wang (2007) ensemble of climate model projections. Shown are the ensemble means of (a) sea surface temperature, (b) surface air temperature, and (c) 850-hPa temperature. The white 5-point stars indicate the region of interest in the present study.

precipitation, Pacific interdecadal climate variability, and its implications for projected climate change in the northeast Pacific Ocean region. The analysis yielded the following conclusions:

1) The water-balance snowpack estimate verified well against observations and represents an alternative to hydrological modeling for producing a historical monthly record of snowpack when high-quality, long-term climate observations of precipitation and streamflow are available.
2) Using the water-balance Cascade snowpack, the overall trend in Cascade spring snowpack over the entire period of record (1930–2007) is −23% of the 1961–90 normal, although this trend does not quite meet the 95% confidence level for a nonzero trend. The trend is primarily a result of warming, as precipitation showed little trend during this period.
3) The loss in snowpack during the period 1950–97, when the PDO shifted from a cool to a warm phase, was a statistically significant 48%, attributable to warming and, to a lesser extent, a decline in precipitation.
4) The spring snowpack trend during the recent period of relatively rapid global temperature increase (1976–2007) was marked by *increasing* Cascade spring snowpack, although the trend is well short of the threshold for statistical significance at the 5% level because of the short time period considered and large annual variability in snowpack.
5) Better correlations of snowpack with temperature and precipitation were obtained, and smaller residual trends remain, when multiple linear regression of snowpack is performed using the winter-mean 850-hPa temperature upwind of the Cascades during onshore flow at that height, rather than the winter-mean surface temperature in the Cascade Mountains. This suggests that the 850-hPa temperature during onshore flow is a key controlling temperature for the phase of Cascade precipitation and the buildup of snowpack. The recent three decades have seen little increase in this temperature parameter, consistent with little change in Cascade snowpack during that period, and the lack of warming of the eastern Pacific.
6) Using the winter-mean temperature at 850 hPa during onshore flow, we estimate the sensitivity of Cascade snowpack to temperature to be approximately $-11 \pm 4\%$ °C^{-1}, somewhat less than the recent estimate by Casola et al. (2009) of -16% °C^{-1}.
7) The large 48% decline in Cascade snowpack between 1950 and 1997 is mostly attributable to natural variability of the North Pacific region. The North Pacific Index (NPI), which is one measure of Pacific atmospheric climate variability, explains less than 50% of this downward trend. However, a new "Cascade Snowpack Circulation" index, that accounts for multiple modes of variability in the winter-mean North Pacific sea level pressure field that most strongly affect Cascade snowpack, explains about 80% of the downward trend in spring snowpack during this period. The residual snowpack time series displays a modest steady loss rate of 2% decade^{-1}. The total residual loss from 1930 to 2007 is 16% and is very nearly statistically significant. An unknown portion of this residual loss may be due to anthropogenic global warming.
8) During the 78-yr record of the water-balance snowpack time series (1930–2007), the dates of maximum

snowpack and 90% melt out both shifted earlier by 5 days. Neither of these shifts is statistically significant.

9) An ensemble of coupled climate model projections for the next several decades projects that the temperatures at 850 hPa over the northeastern Pacific Ocean will warm at a rate of roughly 0.21°C decade^{-1}. Combining this warming rate with our observationally based sensitivity calculation yields a projection that cumulative loss of Cascade spring snowpack from 1985 to 2025 will be 9%, which is considerably less than the 29% loss projected for the same period by a recent climate impacts report for Washington State.

Acknowledgments. We are grateful to Dr. Muyin Wang of NOAA/PMEL/JISAO for providing the coupled GCM ensemble plots of temperature over the Pacific basin. Andrew Wood of the University of Washington and 3Tier, Inc., provided the VIC hydrological simulation climatologies of water-balance terms for Cascade Mountain watersheds. Neal Johnson processed the upper-air sounding data used in this research. We are also grateful to several informal reviewers of an early version of this paper, especially Mike Wallace, Nate Mantua, and Joe Casola, who provided thorough critical reviews. This research was supported by the National Science Foundation, Atmospheric Sciences Division, under Grants 0509079, 0504028, and 0634999, and a grant from Seattle City Light.

APPENDIX

The Water-Balance Snowpack Estimate

a. Methodology

The snowpack estimate is based on a simple water-balance equation for a watershed (or group of watersheds) over some specified time period:

$$\Delta S = P - E - R - \Delta M, \qquad \text{(A1)}$$

where ΔS is the change in snow water equivalent volume, P is precipitation, E is evapotranspiration (or ET), R is runoff (assumed to be equal to gauge-measured streamflow), and ΔM is the change in soil moisture (including groundwater) over the period in question. The goal is to apply this equation on a monthly basis to the watershed subset to obtain monthly ΔS. In terms of direct volume measurements for the watershed subset, only R is available. The west Cascade USHCN stations (Fig. 1) provide an uncalibrated estimate of total precipitation volume in the watersheds P_u, which is not the same as the true precipitation volume in the watersheds

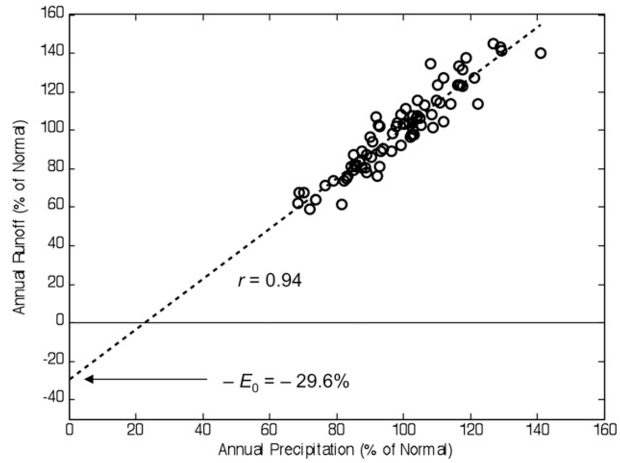

FIG. A1. Scatterplot of annual runoff within the watershed subset (in percent of 1961–90 mean) vs west Cascade-averaged annual precipitation (also in percent of 1961–90 mean). Also shown are the best-fit line, correlation, and y intercept.

P, but is assumed to be proportional to it. Calibration of the precipitation is necessary to account for effects such as the elevation dependence of precipitation, watershed area, and gauge undercatchment. To calibrate P_u, we first consider the application of (A1) to the watershed subset for a full water year (rather than on a monthly time scale). To a good approximation, the annual changes of snowpack and soil moisture are essentially zero, since there is typically little of either remaining at the end of the water year (compared to the maximum amount). Therefore, the annual water balance can be approximated by

$$R = P - E = bP_u - E, \qquad \text{(A2)}$$

where b is the calibration constant that allows the use of the measured Cascade-mean precipitation over the watershed subset. A scatterplot of R (the annual water-year runoff in the watershed subset) versus P_u (Fig. A1) produces a high correlation, 0.94, motivating the use of the linear relationship to calibrate the precipitation. Note that the line does not intersect the origin, and the negative intercept E_0 represents water that does not go into runoff. It would be tempting to simply assume that this constant amount represents the total annual ET. This implies that annual ET is 30% of mean annual runoff. However, long-term hydrological model simulations applied to Cascade watersheds[8] indicate that mean annual ET in

[8] A. Wood (University of Washington) has provided climatological water-balance data from simulations using the VIC hydrologic model within several Cascade Mountain watersheds during the period 1971–2000, described in Wood and Lettenmaier (2006). Those watersheds were similar in location to, but not the same as, the ''watershed subset'' used in the present study.

the Cascades is larger, around 49% of mean annual runoff. To account for this discrepancy within the context of the nearly linear relationship between R and P_u, we define an estimate of ET that includes both E_0 and an additional part that is proportional to annual precipitation:

$$E_{\mathrm{est}} = aP + E_0 = abP_u + E_0. \tag{A3}$$

Substituting this into (A2), applying the result to the 1930–2007 means (overbars) for R and P_u, (i.e., the means of the y and x data points, respectively, in Fig. A1), and assuming the ratio $\eta \equiv \overline{E}/\overline{R} = 0.49$ as suggested above, we obtain

$$b = (1 + \eta)\overline{R}/\overline{P_u} = 1.51 \quad \text{and}$$
$$a = 1 - (\overline{R} + E_0)/(b\overline{P_u}) = 0.131. \tag{A4}$$

These values can then be used to calibrate the annual precipitation ($P = bP_u$). Once the calibrated precipitation volume into the watershed subset is known, a better estimate of annual ET can be obtained by solving (A2) for E. This estimate of ET is equal to the linear fit-based estimate from (A3), minus the annual residual in streamflow (the vertical excursion of each data point from the line in Fig. A1), which importantly includes any long-term trend in annual ET related to warming. In fact, the method yields a small positive trend in ET from 1930 to 2007 that is balanced by a small downward trend in snowpack that is included in the snowpack time series shown in this paper.

To produce the monthly time series, all terms in (A1) must be accounted for. The monthly runoff is known, and the monthly precipitation is assumed to calibrate with the same constant as the annual precipitation [i.e., the b constant, as calculated in (A4)]. Although the annual ET can be estimated with (A3) and (A4), this amount must be distributed among the months of the water year, and an additional assumption must be made about the monthly change in soil moisture. A reasonable approach is to assume that the monthly sum of E and ΔM follows the monthly climatologies of these quantities, multiplied by a constant of proportionality so that the annual total equals the annual total E already calculated (with the annual total of ΔM assumed to be zero, as mentioned previously). We utilize a climatology of these terms (Fig. A2) that was derived from the previously mentioned long-term hydrological model simulations for the Cascades. We tested the sensitivity of the snowpack estimate to other methods, including a simple equal allocation of annual ET among the 12 months (and no accounting for monthly ΔM), and results did not differ substantially, so the method adopted here should not be thought to depend critically on the hydrological model

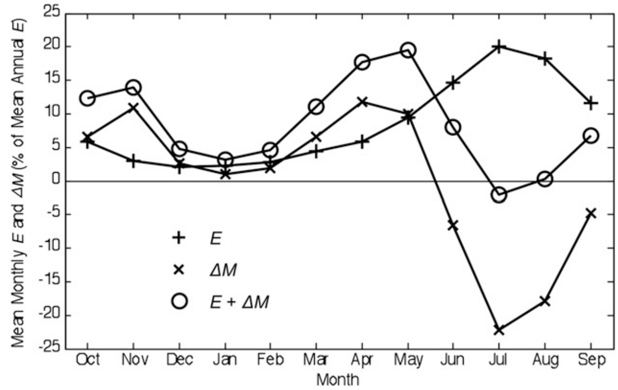

FIG. A2. Climatological monthly values of evapotranspiration (E), change in soil moisture (ΔM), and the sum of the two, expressed as a percentage of the mean annual evapotranspiration, derived from VIC hydrological model simulations for four Cascade Mountain watersheds for the period 1971–2000.

climatology. Rather, it suggests that, at least for the Cascade region considered, variability in precipitation and runoff are dominant over variability in ET and soil moisture in determining the variability in snowpack. It also lends confidence to our approach, which relies on good measurements of the important quantities (precipitation and runoff), and assumptions about the less important ones (ET and soil moisture). Additionally, the finding by Hamlet et al. (2007) that the timing of the ET and soil moisture annual cycles in the Pacific Northwest has not changed substantially since the early twentieth century provides some assurance that our simple method is not missing an important ET–soil moisture-dependent contribution to climatic changes in the Cascades water balance.

With monthly values of all of the terms in (A1), and assuming the snowpack starts out at zero in each water year, (A1) is integrated in monthly increments to obtain a value of SWE volume at the end of each month. The monthly values are then converted to percent of the 1961–90 mean 1 April value, yielding the final monthly time series of snowpack within the watershed subset for the period 1930–2007.

b. Uncertainty and its implications for results

There are several sources of uncertainty that enter into our water-balance-based estimate of Cascade snowpack. The streamflow and precipitation measurements, although quality controlled, contain errors. The linear regression between annual runoff and annual precipitation that is used to calibrate watershed precipitation is high ($r = 0.94$) but not perfect. Although ET is allowed to vary on an annual basis, there is an assumed form of the annual cycle, which introduces error in the monthly snowpack time series. Indeed, there are likely other sources of error that are difficult to identify, let alone quantify.

Rather than attempt to quantify all the separate sources of error, we make use of Fig. 3 to estimate the overall error of the method. The remaining variance in the directly measured snow course snowpack that is unexplained by the linear fit to the water-balance snowpack provides an estimate of this error. However, the snow course snowpack is also prone to error, and considering that the two estimates use entirely different data sources that are not collocated, it is most likely that the errors in the two estimates are uncorrelated. Therefore the residual variance contains contributions from uncorrelated errors in both estimates and is thus an overestimate of the error in either method separately. Nevertheless, we use this residual variance as a liberal estimate of the error in the water-balance snowpack (i.e., the true error is probably less than this estimate). Additionally and importantly, the residual is essentially uncorrelated with time and with snowpack amount.

The residual variance is $(11\%)^2$ (i.e., 121 ''squared percent'' of the 1961–90 mean snowpack). To quantify how this uncertainty affects the confidence intervals in the snowpack trends shown in Figs. 5a and 8c, we can combine the variance of the estimated error with that of the full annual time series to obtain a new, larger confidence interval. The Bienaymé formula states that the variance of the sum of two uncorrelated variables is the sum of their variances; that is, $\sigma^2_{\mathrm{annvar+error}} = \sigma^2_{\mathrm{annvar}} + \sigma^2_{\mathrm{error}}$, where $\sigma^2_{\mathrm{annvar}}$ is the variance of the detrended annual time series shown in Fig. 5a or 8c, and $\sigma^2_{\mathrm{error}}$ is the residual variance of $(11\%)^2$ mentioned above. Since the Casola et al. (2009) formula for the confidence interval is directly proportional to standard deviation, the adjustment factor for the confidence intervals already calculated is $f = \sqrt{(\sigma^2_{\mathrm{annvar}} + \sigma^2_{\mathrm{error}})/\sigma^2_{\mathrm{annvar}}}$. The values of $\sigma^2_{\mathrm{annvar}}$ from Figs. 5a and 8c are $(36\%)^2$ and $(19\%)^2$, respectively, yielding adjustment factors of 1.05 and 1.17, respectively. In other words, all the confidence intervals in Fig. 5a should be multiplied by 1.05, and in Fig. 8c by 1.17, to account for the estimated error. Both of these factors are only slightly larger than 1.0. In the case of the full snowpack time series (Fig. 5a), it has no impact on the significance of the trends shown. In the case of the snowpack time series after removal of the influence of the CSC index (Fig. 8c), the factor causes the 1930–2007 trend to switch from being slightly larger than the confidence interval to slightly smaller. Considering the arbitrary choice of a 95% confidence level, it is probably best to describe this trend as ''very nearly'' statistically significant.

The above analysis does not translate well to the time series of dates of maximum snowpack and melt out (Fig. 9), because they are fundamentally different quantities. However, it is likely that inclusion of methodological error would make these trends somewhat less significant than they already are, having no qualitative effect on the conclusions.

REFERENCES

Allan, R., and T. Ansell, 2006: A new globally complete monthly historical gridded mean sea level pressure dataset (HadSLP2): 1850–2004. *J. Climate,* **19,** 5816–5842.

Barnett, T. P., and Coauthors, 2008: Human-induced changes in the hydrology of the western United States. *Science,* **319,** 1080–1083.

Brohan, P., J. J. Kennedy, I. Harris, S. F. B. Tett, and P. D. Jones, 2006: Uncertainty estimates in regional and global observed temperature changes: A new dataset from 1850. *J. Geophys. Res.,* **111,** D12106, doi:10.1029/2005JD006548.

Casola, J. H., L. Cuo, B. Livneh, D. P. Lettenmaier, M. T. Stoelinga, P. W. Mote, and J. M. Wallace, 2009: Assessing the impacts of global warming on snowpack in the Washington Cascades. *J. Climate,* **22,** 2758–2772.

Cayan, D. R., 1996: Interannual climate variability and snowpack in the western United States. *J. Climate,* **9,** 928–948.

——, S. A. Kammerdiener, M. D. Dettinger, J. M. Caprio, and D. H. Peterson, 2001: Changes in the onset of spring in the western United States. *Bull. Amer. Meteor. Soc.,* **82,** 399–415.

Dodson, M., and Coauthors, 2004: Oregon strategy for greenhouse gas reductions. Oregon Department of Energy, 192 pp.

Durre, I., R. S. Vose, and D. B. Wuertz, 2006: Overview of the Integrated Global Radiosonde Archive. *J. Climate,* **19,** 53–68.

Elsner, M. M., and Coauthors, 2009: Implications of 21st century climate change for the hydrology of Washington State. *The Washington Climate Change Impacts Assessment,* J. Littell et al., Eds., Climate Impacts Group, University of Washington, 69–106.

Guilyardi, E., 2006: El Niño–mean state–seasonal cycle interactions in a multi-model ensemble. *Climate Dyn.,* **26,** 329–348.

Hamlet, A. F., P. W. Mote, M. P. Clark, and D. P. Lettenmaier, 2005: Effects of temperature and precipitation variability on snowpack trends in the western United States. *J. Climate,* **18,** 4545–4561.

——, ——, ——, and ——, 2007: Twentieth-century trends in runoff, evapotranspiration, and soil moisture in the western United States. *J. Climate,* **20,** 1468–1486.

Hansen, J., R. Ruedy, M. Sato, M. Imhoff, W. Lawrence, D. Easterling, T. Peterson, and T. Karl, 2001: A closer look at United States and global surface temperature change. *J. Geophys. Res.,* **106** (D20), 23 947–23 963.

Karl, T. R., C. N. Williams Jr., F. T. Quinlan, and T. A. Boden, 1990: United States Historical Climatology Network (HCN) serial temperature and precipitation data. Carbon Dioxide Information and Analysis Center, Environmental Science Division Publication 3404, Oak Ridge Laboratory, 389 pp.

Lettenmaier, D. P., 1976: Detection of trends in water quality data from records with dependent observations. *Water Resour. Res.,* **12,** 1037–1046.

Liang, X., D. P. Lettenmaier, E. F. Wood, and S. J. Burges, 1994: A simple hydrologically based model of land surface water and energy fluxes for general circulation models. *J. Geophys. Res.,* **99** (D7), 14 415–14 428.

Mantua, N. J., S. R. Hare, Y. Zhang, J. M. Wallace, and R. C. Francis, 1997: A Pacific interdecadal climate oscillation with impacts on salmon production. *Bull. Amer. Meteor. Soc.,* **78,** 1069–1079.

Meehl, G. A., A. Hu, and B. D. Santer, 2009: The mid-1970s climate shift in the Pacific and the relative roles of forced versus inherent decadal variability. *J. Climate,* **22,** 780–792.

Minder, J. R., 2010: The sensitivity of mountain snowpack accumulation to climate warming. *J. Climate,* **23,** 2634–2650.

Mote, P. W., 2003: Trends in snow water equivalent in the Pacific Northwest and their climatic causes. *Geophys. Res. Lett.,* **30,** 1601, doi:10.1029/2003GL017258.

——, 2006: Climate-driven variability and trends in mountain snowpack in western North America. *J. Climate,* **19,** 6209–6220.

——, A. F. Hamlet, M. P. Clark, and D. P. Lettenmaier, 2005: Declining mountain snowpack in western North America. *Bull. Amer. Meteor. Soc.,* **86,** 39–49.

——, ——, and E. Salathé, 2008: Has spring snowpack declined in the Washington Cascades? *Hydrol. Earth Syst. Sci.,* **12,** 193–206.

Overland, J. E., and M. Wang, 2007: Future climate of the North Pacific Ocean. *Eos, Trans. Amer. Geophys. Union,* **88,** doi:10.1029/2007EO160003.

Panofsky, H. A., and G. W. Brier, 1963: *Some Applications of Statistics to Meteorology*. The Pennsylvania State University, 224 pp.

Pierce, D. W., and Coauthors, 2008: Attribution of declining western U.S. snowpack to human effects. *J. Climate,* **21,** 6425–6444.

Regonda, S. K., B. Rajagopalan, M. Clark, and J. Pitlick, 2005: Seasonal cycle shifts in hydroclimatology over the western United States. *J. Climate,* **18,** 372–384.

Slack, J. R., and J. M. Landwehr, 1992: Hydro-climatic data network (HCDN): A U.S. Geological Survey streamflow data set for the United States for the study of climate variations, 1874–1988. U.S. Geological Survey Open-File Rep. 92-129, 193 pp.

Solomon, S., D. Qin, M. Marquis, K. Averyt, M. Tignor, and H. L. Miller, Eds., 2007: *Climate Change 2007: The Physical Science Basis*. Cambridge University Press, 996 pp.

Stewart, I. T., D. R. Cayan, and M. D. Dettinger, 2005: Changes toward earlier streamflow timing across western North America. *J. Climate,* **18,** 1136–1155.

Trenberth, K. E., and J. W. Hurrell, 1994: Decadal atmosphere-ocean variations in the Pacific. *Climate Dyn.,* **9,** 303–319.

van den Dool, H., 2007: *Empirical Methods in Short-Term Climate Prediction.* Oxford University Press, 215 pp.

Wallace, J. M., and D. S. Gutzler, 1981: Teleconnections in the geopotential height field during the Northern Hemisphere winter. *Mon. Wea. Rev.,* **109,** 784–812.

Wood, A. W., and D. P. Lettenmaier, 2006: A test bed for new seasonal hydrologic forecasting approaches in the western U.S. *Bull. Amer. Meteor. Soc.,* **87,** 1699–1712.